nature biotechnology

RNA processing enables predictable programming of gene expression

Lei Qi[1,7], Rachel E Haurwitz[2,7], Wenjun Shao[2], Jennifer A Doudna[2–5] & Adam P Arkin[1,5,6]

Complex interactions among genetic components often result in variable systemic performance in designed multigene systems[1,2]. Using the bacterial clustered regularly interspaced short palindromic repeat (CRISPR) pathway[3,4] we develop a synthetic RNA-processing platform, and show that efficient and specific cleavage of precursor mRNA enables reliable and predictable regulation of multigene operons. Physical separation of linked genetic elements by CRISPR-mediated cleavage is an effective strategy to achieve assembly of promoters, ribosome binding sites, *cis*-regulatory elements, and riboregulators into single- and multigene operons with predictable functions in bacteria. We also demonstrate that CRISPR-based RNA cleavage is effective for regulation in bacteria, archaea and eukaryotes. Programmable RNA processing using CRISPR offers a general approach for creating context-free genetic elements and can be readily used in the bottom-up construction of increasingly complex biological systems in a plug-and-play manner.

Genetic systems often behave unpredictably as a result of structural interactions between DNA, RNA and protein components as well as functional interactions with host factors and metabolites[1]. Owing to these complexities, our ability to quantitatively program multigenic circuits and metabolic pathways based on the characteristics of individual components is very limited. Transcription, translation and degradation of an RNA transcript are crucial in gene expression[5], and all three events are controlled by a combination of promoters, ribosome binding sites (RBSs) and *cis*-regulatory signals that are encoded in untranslated regions (UTRs)[2]. These elements can unpredictably interact with each other through the formation of RNA structures and the recruitment of factors that can affect global transcript accessibility and stability. We hypothesized that physically separating genetic elements at the transcript level might facilitate modular programming of predictable genetic systems.

To test this hypothesis, we used a synthetic RNA-processing platform derived from the CRISPR system. CRISPRs are widespread in bacteria and archaea, and confer resistance to invasive genetic elements[4,6]. The CRISPR locus is transcribed into a long precursor RNA (pre-crRNA) that contains repetitive sequence elements[7–10]. A dedicated CRISPR-associated (Cas) endoRNase cleaves the pre-crRNA in each repetitive element, generating short crRNAs necessary for protection against invaders[3,11–13]. In *Pseudomonas aeruginosa* strain UCBPP-PA14, the single endoRNase Csy4 recognizes and cleaves a 28-nucleotide (nt) repetitive sequence[3] (**Supplementary Fig. 1**) and produces stable transcripts with a 5′ hydroxyl group[14] (**Supplementary Fig. 2**). Our synthetic cleavage platform comprises the *csy4* gene and its cleavage element. The cleavage element is inserted into reporter transcripts between other components, and the Csy4 protein is induced to cleave at designed loci and generate well-defined RNA segments. Csy4 is highly specific for its cognate RNA target and does not recognize other types of CRISPR sites such as those present in the *Escherichia coli* K12 chromosome[3] and is therefore well-suited for use as a synthetic platform.

We first constructed two reporter libraries in *E. coli* to test whether RNA cleavage could eliminate unwanted interactions between UTRs and translational elements such as RBSs. In the control library, we placed random 30-nt UTR sequences between a constitutive promoter and a characterized RBS that we fused to a superfolder GFP–coding gene. In the CRISPR library, we inserted the 28-nt CRISPR hairpin between the random UTRs and the RBS. The protein production rates in clones that we randomly sampled from each library (45 clones) were measured during exponential cell growth (**Fig. 1a**). The control library exhibited an almost threefold wider distribution of protein production rates than the CRISPR library as measured by the relative standard deviation (RSD of 46% and 19%, respectively; **Fig. 1b**,**c**). The difference in mean expression between the control library and a baseline construct lacking the 30-nt UTR insertion (baseline bias of 0.44) was larger than that of the CRISPR library (baseline bias of 0.19). We observed that both RSD and baseline bias increased in the absence of Csy4 expression (**Fig. 1d**). Expression of Csy4 together with the cleavage element led to a reduction in the size of the transcript as detected by northern blotting, consistent with cleavage of mRNA at the CRISPR hairpin (**Supplementary Fig. 3**). Similar experiments with inserted random 30-nt UTRs between different RBSs and genes with the cleavage element exhibited a consistent reduction in expression variability and baseline bias compared to those without the cleavage element (**Supplementary Fig. 4**). As genomic 5′ UTRs have variable lengths and encode a variety of structures that might not be represented in the random library, we tested in the same

[1]Department of Bioengineering, University of California Berkeley, Berkeley, California, USA. [2]Department of Molecular and Cell Biology, University of California Berkeley, Berkeley, California, USA. [3]Howard Hughes Medical Institute, University of California Berkeley, Berkeley, California, USA. [4]Department of Chemistry, University of California, Berkeley, Berkeley, California, USA. [5]Physical Biosciences Division, Lawrence Berkeley National Laboratory, Berkeley, California, USA. [6]California Institute for Quantitative Biosciences (QB3), Berkeley, California, USA. [7]Present addresses: Center for Systems and Synthetic Biology, University of California San Francisco, San Francisco, California, USA (L.Q.) and Caribou Biosciences, Inc., Berkeley, California, USA. (R.E.H.). Correspondence should be addressed to A.P.A. (aparkin@lbl.gov).

Received 29 March; accepted 7 August; published online 16 September 2012; doi:10.1038/nbt.2355

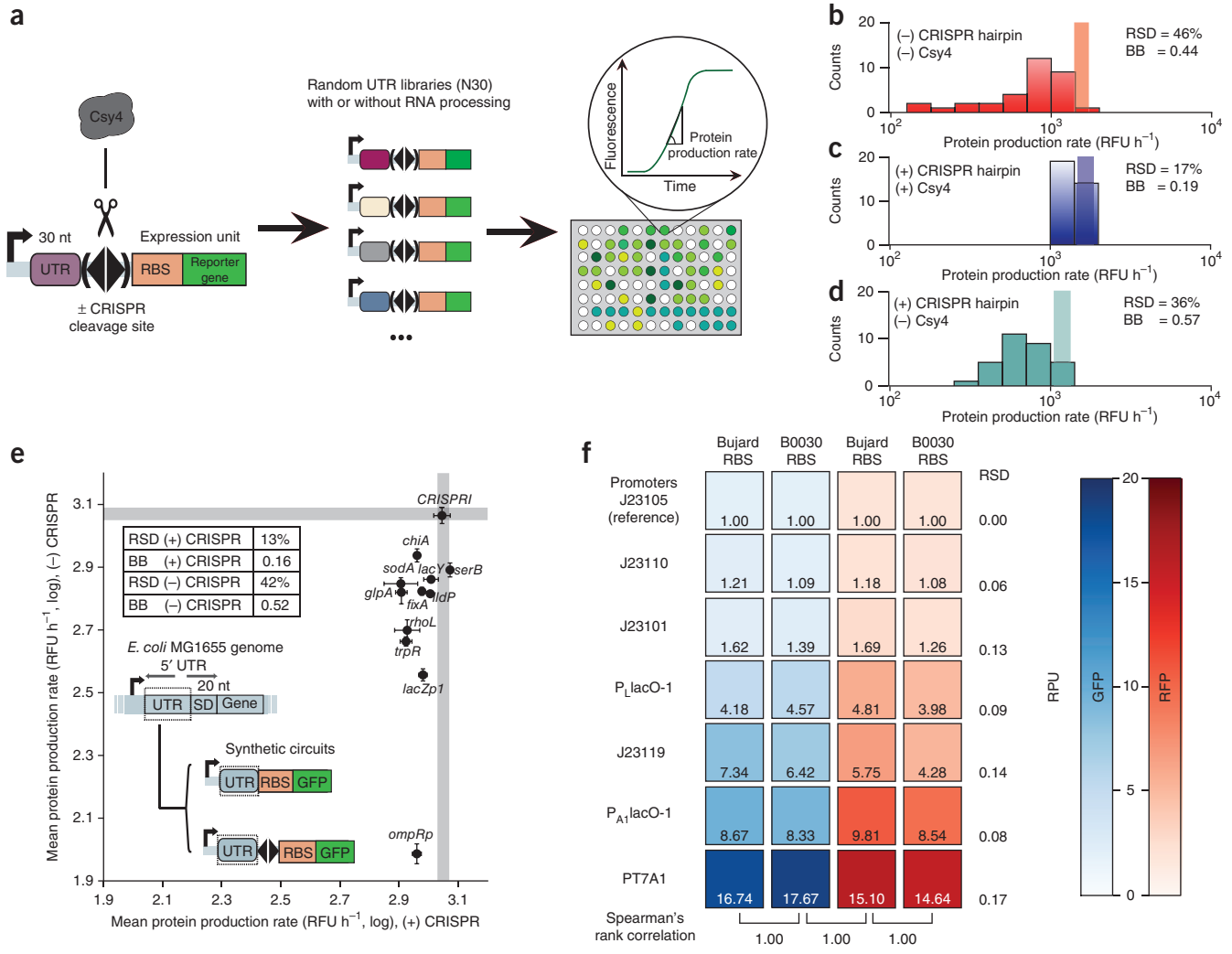

Figure 1 The CRISPR RNA-processing system allows engineering of standard genetic elements in various contexts. (**a**) Experimental procedure for measuring the effects of random UTRs on gene expression with and without the CRISPR cleavage element (diamond). (**b**–**d**) Statistical analysis of protein production rates (BB, baseline bias). Expression data for baseline constructs without 30-nt UTR insertions are plotted as unbounded shaded bars, with the width representing the s.d. of biological triplicates. (**e**) Mean protein production rates for 12 genomic UTR insertions with and without RNA processing. Gray lines indicate protein production for the baseline constructs. (**f**) Experimental data for 28 combinatory circuits composed of 7 promoters, 2 RBSs and 2 reporter genes with the cleavage element inserted between promoters and RBSs. Heatmaps show RPU values, with each column normalized to a reference promoter J23105. The RSD values for each row and Spearman's rank correlation coefficients between adjacent columns are labeled. In all cases, $P < 0.0001$ ($n = 7$) for the differences in RSD and baseline bias using two-tailed Student's *t*-test.

reporter system 12 different 18–90-nt UTR sequences present in the *E. coli* MG1665 genome. Consistent with results obtained in the random library, we observed much lower variation in protein production rates with RNA cleavage compared to that observed without it (**Fig. 1e**), implying that RNA processing enabled predictable gene expression regardless of UTR context.

Most promoters used in synthetic biology and metabolic engineering are derived from natural DNA sequences, usually with poorly annotated operator sequences and transcriptional start sites[15]. As a consequence, assembling promoters with UTR, RBS and coding sequence elements often modifies transcript composition, which changes translational efficiency and transcript stability, and alters the putative activity of the promoter in different contexts, in an unpredictable fashion. To determine whether RNA processing could reduce the interference among gene expression control elements, we compared two expression libraries with and without RNA cleavage. Both libraries consisted of 28 parallel constructs generated by combinatorial assembly of seven promoters with two RBSs and two reporter genes (**Supplementary Methods**). We inserted the cleavage element between the promoters and RBSs in the CRISPR library and assayed the relative promoter unit (RPU) of each promoter by normalizing its protein production rate to that for a reference promoter. The measured RPU values in the control library varied widely across different RBSs and genes (RSD values of 67% to ~129%, **Supplementary Fig. 5**). In contrast, the RPU value of each promoter in the CRISPR library was almost constant, and the rank orders were completely conserved across different contexts (**Fig. 1f**). This shows that cleavage of the mRNA between promoters and downstream elements enabled production of standard RPU values from promoters, which could then be used predictably in complex genetic systems in a plug-and-play manner.

We applied RNA processing to the rational design of multigene operons. In bacteria, archaea[16] and eukaryotes[17], multigene operons

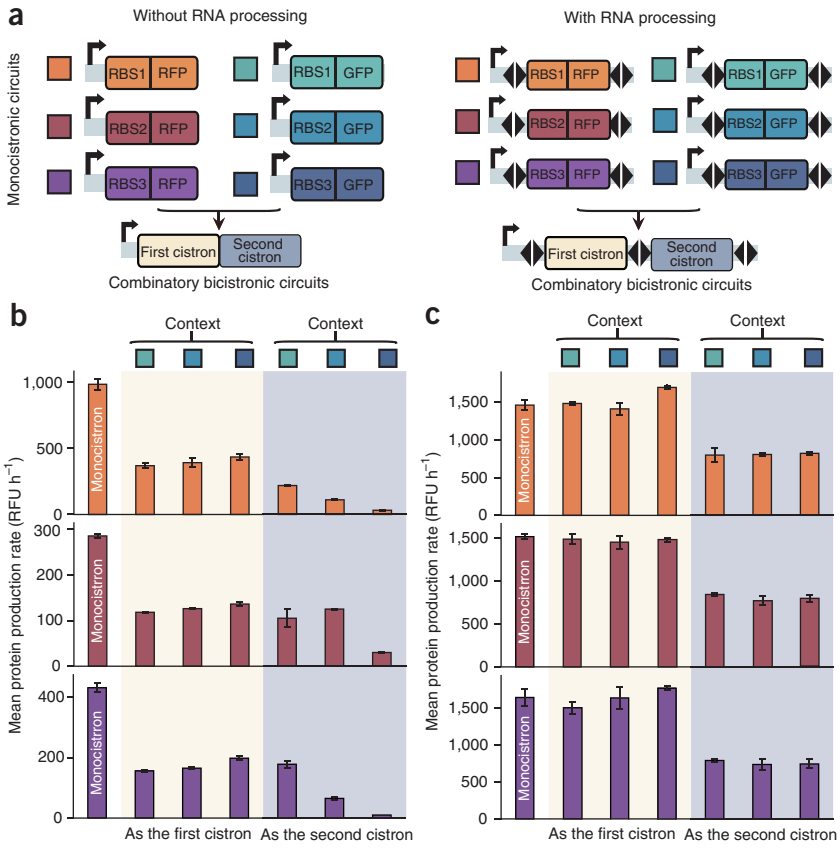

Figure 2 RNA processing enables design of operonic systems. (**a**) Six monocistrons were combined in pairs to generate eighteen bicistrons without (left) and with (right) cleavage elements (**Supplementary Methods**). (**b**) Measured protein production rates (PPRs) for the monocistrons and bicistrons without RNA processing. The first bar in each graph shows the measured PPR for the monocistron. The measured PPRs for bicistrons with RFP in the first and second cistrons are shaded in yellow and blue. The context is labeled on the top. (**c**) Measured PPRs with RNA processing. The absolute values are different compared to those in **b**. RFU, relative fluorescence units. All error bars indicate s.d. of biological triplicates.

are ubiquitous and enable genome compactness, coordinated regulation, and improved dynamics of transcription and growth[17]. Owing to the advantages of multigene operons, engineering such operons with predictable behaviors has been a focus in metabolic engineering applications[18,19]. However, multiple genes encoded on the same transcript can interfere with one another because of RNA structures and translational coupling, which affects both transcript stability and translation efficiency. We measured and compared protein expression of a set of genes in a monocistron format with different gene arrangements in bicistronic operons, in which cistrons were (or were not) bounded by the CRISPR cleavage elements at both 5′ and 3′ ends to remove context interference from either side. We constructed six monocistrons by combining three RBSs with two fluorescent protein genes, and we constructed the bicistrons by pairing every *RFP* monocistron with all the *GFP* monocistrons such that both *RFP* and *GFP* serve as the first and second gene in the operon. This provided two parallel sets of 18 bicistrons: one without and one with RNA processing (**Fig. 2a**). In the control library, which lacked cleavage elements, expression of the first cistron linearly correlated with monocistron expression, but expression of the second cistron was highly variable (**Fig. 2b**). The results from the CRISPR library were notably different. If a gene was the first cistron in a bicistronic operon, gene expression was almost the same as for the corresponding monocistron; if a gene appeared as the second cistron, there was a strong linear correlation between its expression and that of the corresponding monocistron (**Fig. 2c** and **Supplementary Fig. 6**). The consistent difference in the expression of the second cistron reflects transcriptional polarity[20], an effect that results in reduced expression of operon genes that are distal to the promoter compared with proximal genes. Notably, our synthetic cleavage system allows precise measurement of the RNA polymerase dropoff rate during elongation, which we estimated as 8×10^{-4} per nucleotide in our constructs (**Supplementary Methods** and **Supplementary Fig. 7**).

We next used the CRISPR RNA processing platform to design complex regulatory systems. We used two families of antisense RNA–mediated *cis* elements to achieve multi-input regulation from two orthogonal pairs of translational repressors (IS10wt and IS10-9)[21] and one transcriptional attenuator (PT181wt)[22]. Attempts to use orthogonal intergenic IS10 UTR elements to differentially control translation of individual genes inside an operon failed likely owing to coupled transcript stability and structural interactions between the two cistrons. However, when the precursor transcript was cleaved at designed loci to free the 5′ and 3′ ends, each antisense RNA individually repressed the cognate UTR–gene cassette without affecting the other (**Fig. 3a** and **Supplementary Fig. 8**). This suggests that RNA processing might decouple transcript stability and remove structural interactions between multiple genes and associated regulatory elements on the same transcript. We also designed complex RNA-level regulation by combining two *cis*-regulatory systems, PT181wt and IS10wt, in tandem to control a monocistron. Ideally, such tandem multi-input control would result in a multiplicative function of the two elements[22]. Without RNA cleavage, this outcome was not obtained. With RNA cleavage. we achieved multiplicative regulation, which is crucial to the design of sophisticated and quantitatively predictable RNA-level genetic circuits (**Fig. 3b**), indicating that RNA processing facilitated complex *cis* regulation. We also compared the efficiency of CRISPR-mediated cleavage to cleavage by different RNA-processing elements by inserting different elements into the complex *cis*-regulatory system, including sequence for a satellite tobacco ringspot virus hammerhead ribozyme[23], sequence for an avocado sunblotch virus ribozyme[24], an RNase III binding site (R1.1) from T7 phage[25] and a tRNA sequence for Arg5 (ref. 26) (**Fig. 3c**). None of these elements was as effective at tuning gene expression as the CRISPR system. This result might indicate that the CRISPR system is robust to different genetic contexts, and this could be a unique feature of the CRISPR system, as Csy4 naturally cleaves its RNA target in a variety of context sequences derived from phage genomes[4].

Csy4 functions in a wide spectrum of bacteria, archaea and eukaryotes. Using a reporter system in which the Cys4 cleavage site was inserted in-frame between the translation start codon and downstream protein-coding sequence, we showed that Csy4 cleavage led to effective gene silencing with more than tenfold on-off dynamic range in the gram-negative bacterium *E. coli*, the gram-positive

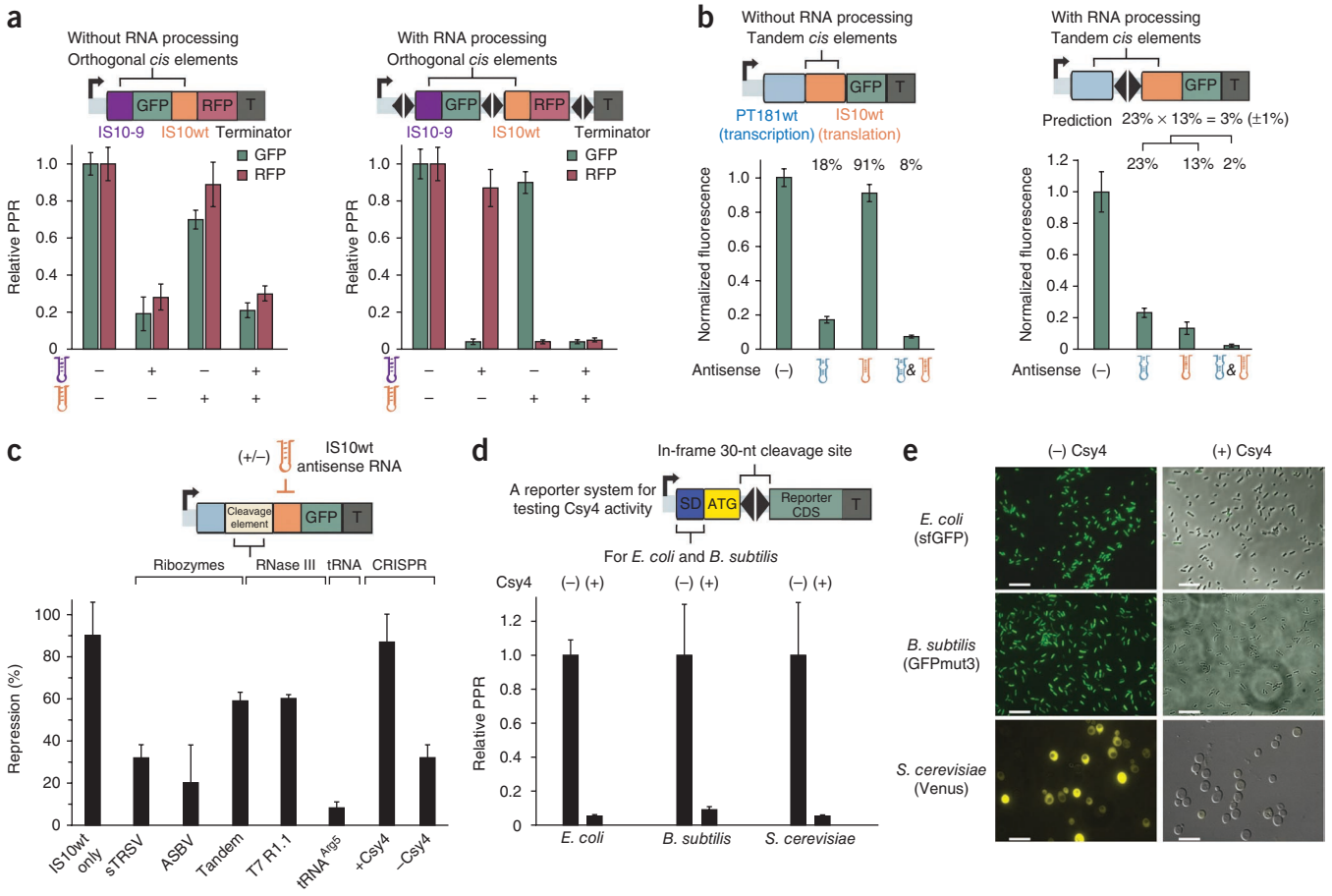

Figure 3 Applications of CRISPR RNA processing to the predictable engineering of complex regulatory systems. (**a**) Schematics of orthogonally acting IS10 antisense RNA-mediated intergenic UTR elements used to control translation of individual genes in an operon without (left) or with (right) RNA processing (top). T, transcription terminator. Calculated relative protein production rates (PPRs) were normalized to the case without any antisense RNA (bottom). Antisense RNAs are represented as hairpins: IS10wt (orange), IS10-9 (purple) and PT181wt (blue). (**b**) Schematics of a tandem *cis*-regulatory system without (left) or with (right) RNA processing (top). Data were normalized to gene expression without any antisense RNA. (**c**) Efficacy of different RNA-cleavage elements inserted between the tandem *cis* regulators (PT181wt and IS10wt). sTRSV, satellite tobacco ringspot virus hammerhead ribozyme; ASBV, avocado sunblotch virus ribozyme, T7 R1.1, the RNase III binding site from T7 phage; $tRNA^{Arg5}$, tRNA sequence for Arg5 (**Supplementary Methods**). (**d**) Relative protein production rates when the 30-nt Csy4 cleavage site was inserted in-frame into a reporter system between the ATG start codon and downstream protein coding sequence. The reporter systems were tested without and with Csy4 co-expression in the indicated organisms. SD, Shine-Dalgarno sequence; CDS, coding sequence. All error bars indicate s.d. of biological triplicates. (**e**) Fluorescence images of *E. coli*, *B. subtilis* and *S. cerevisiae* cells without and with Csy4 expression. All cells express their reporter systems without (left) and with (right) Csy4 expression. Scale bars, 10 μm.

bacterium *Bacillus subtilis* and the eukaryote *Saccharomyces cerevisiae* (**Fig. 3d**,**e**). This suggests that the RNA-processing platform based on Csy4 has the potential to be readily expanded to different organisms to build predictable genetic systems with dynamic controls.

Our results show that RNA processing is an effective strategy to maintain the relative strengths of promoters in different genetic contexts, avoid interference between genes in multigenic operons and enable predictable performance of tandem or intergenic regulatory elements in untranslated regions of the transcript. RNA cleavage enables high levels of modularity between otherwise physically linked and functionally coupled elements and provides an attractive solution to the creation of physically and functionally standard, context-free promoters, RBSs and UTRs. Regularized genetic elements with well-defined quantitative functions can complement library-based approaches for optimizing multigene circuits[27] and metabolic pathways[18], wherein the predictable quantitative function of individual control elements allows forward design of a uniform coverage of expression parameter space with a smaller set of well-chosen combinations of parts. Such designed library screens could map parts to parameters and parameters to performance (for example, productivity of a metabolic pathway), making it possible to infer untested parameter combinations to improve systemic performance. Such 'design of experiments' approaches are promising for more rapid and cost-effective engineering of increasingly complex biological systems[28].

Our choice of the Csy4 cleavage platform recapitulates the highly specific and efficient RNase activity of the CRISPR system, and we found it to be more effective than other cleavage elements including hammerhead ribozymes and RNase III. Existence of many Csy4 homologs from other independent CRISPR-Cas systems will potentially enable the specific cleavage of distinct RNA targets, which opens the possibility of programming RNA processing and editing in a parallel manner[4]. We showed that Csy4 cleavage is fully functional in different organisms including yeast, suggesting the universality of this platform across the kingdoms of life. Together with technologies for

genome-scale modification[29], this study establishes a foundation for applications including creation of standardized promoters and UTR elements, engineering of differently regulated metabolic pathways and design of predictable complex genetic programs for cell therapies, chemical production and cellular computation.

METHODS

Methods and any associated references are available in the online version of the paper.

Note: Supplementary information is available in the online version of the paper.

ACKNOWLEDGMENTS

We thank members of BIOFAB, International Open Facility Advancing Biotechnology, for distributing genetic parts, and J. Dueber, M. Lee and H. Lee (University of California, Berkeley) for providing the yeast vector. This work was supported by the US National Science Foundation (SynBERC, NSFEEC-0540879, L.Q. and A.P.A.), Department of Energy through Laboratory Directed Research and Development (DE-AC02-05CH11231d, L.Q., W.S. and A.P.A.) and Howard Hughes Medical Institute (R.E.H. and J.A.D.).

AUTHOR CONTRIBUTIONS

L.Q., A.P.A. and J.A.D. conceived of the research; L.Q., R.E.H., W.S., J.A.D. and A.P.A. designed the study; L.Q., R.E.H. and W.S. performed the experiments; L.Q., R.E.H., J.A.D. and A.P.A. analyzed the data and wrote the manuscript.

COMPETING FINANCIAL INTERESTS

The authors declare competing financial interests: details are available in the online version of the paper.

Published online at http://www.nature.com/doifinder/10.1038/nbt.2355.
Reprints and permissions information is available online at http://www.nature.com/reprints/index.html.

1. Ellis, T., Wang, X. & Collins, J.J. Diversity-based, model-guided construction of synthetic gene networks with predicted functions. *Nat. Biotechnol.* **27**, 465–471 (2009).
2. Endy, D. Foundations for engineering biology. *Nature* **438**, 449–453 (2005).
3. Haurwitz, R.E., Jinek, M., Wiedenheft, B., Zhou, K. & Doudna, J.A. Sequence- and structure-specific RNA processing by a CRISPR endonuclease. *Science* **329**, 1355–1358 (2010).
4. Wiedenheft, B., Sternberg, S.H. & Doudna, J.A. RNA-guided genetic silencing systems in bacteria and archaea. *Nature* **482**, 331–338 (2012).
5. Culler, S.J., Hoff, K.G. & Smolke, C.D. Reprogramming cellular behavior with RNA controllers responsive to endogenous proteins. *Science* **330**, 1251–1255 (2010).
6. Barrangou, R. *et al.* CRISPR provides acquired resistance against viruses in prokaryotes. *Science* **315**, 1709–1712 (2007).
7. Al-Attar, S., Westra, E.R., van der Oost, J. & Brouns, S.J.J. Clustered regularly interspaced short palindromic repeats (CRISPRs): the hallmark of an ingenious antiviral defense mechanism in prokaryotes. *Biol. Chem.* **392**, 277–289 (2011).
8. Karginov, F.V. & Hannon, G.J. The CRISPR system: small RNA-guided defense in bacteria and archaea. *Mol. Cell* **37**, 7–19 (2010).
9. Gesner, E.M., Schellenberg, M.J., Garside, E.L., George, M.M. & Macmillan, A.M. Recognition and maturation of effector RNAs in a CRISPR interference pathway. *Nat. Struct. Mol. Biol.* **18**, 688–692 (2011).
10. Sashital, D.G., Jinek, M. & Doudna, J.A. An RNA-induced conformational change required for CRISPR RNA cleavage by the endoribonuclease Cse3. *Nat. Struct. Mol. Biol.* **18**, 680–687 (2011).
11. Lintner, N.G. *et al.* Structural and functional characterization of an archaeal clustered regularly interspaced short palindromic repeat (CRISPR)-associated complex for antiviral defense (CASCADE). *J. Biol. Chem.* **286**, 21643–21656 (2011).
12. Carte, J., Pfister, N.T., Compton, M.M., Terns, R.M. & Terns, M.P. Binding and cleavage of CRISPR RNA by Cas6. *RNA* **16**, 2181–2188 (2010).
13. Brouns, S.J.J. *et al.* Small CRISPR RNAs guide antiviral defense in prokaryotes. *Science* **321**, 960–964 (2008).
14. Deana, A., Celesnik, H. & Belasco, J.G. The bacterial enzyme RppH triggers messenger RNA degradation by 5′ pyrophosphate removal. *Nature* **451**, 355–358 (2008).
15. Cases, I. & de Lorenzo, V. Promoters in the environment: transcriptional regulation in its natural context. *Nat. Rev. Microbiol.* **3**, 105–118 (2005).
16. Rocha, E.P.C. The organization of the bacterial genome. *Annu. Rev. Genet.* **42**, 211–233 (2008).
17. Zaslaver, A., Baugh, L.R. & Sternberg, P.W. Metazoan operons accelerate recovery from growth-arrested states. *Cell* **145**, 981–992 (2011).
18. Pfleger, B.F., Pitera, D.J., Smolke, C.D. & Keasling, J.D. Combinatorial engineering of intergenic regions in operons tunes expression of multiple genes. *Nat. Biotechnol.* **24**, 1027–1032 (2006).
19. Martin, V., Pitera, D., Withers, S. & Newman, J. Engineering a mevalonate pathway in *Escherichia coli* for production of terpenoids. *Nat. Biotechnol.* **21**, 796–802 (2003).
20. Wek, R.C., Sameshima, J.H. & Hatfield, G.W. Rho-dependent transcriptional polarity in the ilvGMEDA operon of wild-type *Escherichia coli* K12. *J. Biol. Chem.* **262**, 15256–15261 (1987).
21. Mutalik, V.K., Qi, L., Guimaraes, J.C., Lucks, J.B. & Arkin, A.P. Rationally designed families of orthogonal RNA regulators of translation. *Nat. Chem. Biol.* **8**, 447–454 (2012).
22. Lucks, J.B., Qi, L., Mutalik, V.K., Wang, D. & Arkin, A.P. Versatile RNA-sensing transcriptional regulators for engineering genetic networks. *Proc. Natl. Acad. Sci. USA* **108**, 8617–8622 (2011).
23. Hampel, A. & Tritz, R. RNA catalytic properties of the minimum (–)sTRSV sequence. *Biochemistry* **28**, 4929–4933 (1989).
24. Daròs, J.A., Marcos, J.F., Hernández, C. & Flores, R. Replication of avocado sunblotch viroid: evidence for a symmetric pathway with two rolling circles and hammerhead ribozyme processing. *Proc. Natl. Acad. Sci. USA* **91**, 12813–12817 (1994).
25. Dunn, J.J. & Studier, F.W. T7 early RNAs and *Escherichia coli* ribosomal RNAs are cut from large precursor RNAs in vivo by ribonuclease 3. *Proc. Natl. Acad. Sci. USA* **70**, 3296–3300 (1973).
26. Espéli, O., Moulin, L. & Boccard, F. Transcription attenuation associated with bacterial repetitive extragenic BIME elements1. *J. Mol. Biol.* **314**, 375–386 (2001).
27. Guet, C.C., Elowitz, M.B., Hsing, W. & Leibler, S. Combinatorial synthesis of genetic networks. *Science* **296**, 1466–1470 (2002).
28. Salis, H.M., Mirsky, E.A. & Voigt, C.A. Automated design of synthetic ribosome binding sites to control protein expression. *Nat. Biotechnol.* **27**, 946–950 (2009).
29. Wang, H.H. *et al.* Programming cells by multiplex genome engineering and accelerated evolution. *Nature* **460**, 894–898 (2009).

ONLINE METHODS

Strains and media. The *E. coli* strain Top10 (Invitrogen) was used in all experiments. EZ rich defined medium (EZ-RDM, Teknoka) was used as the growth medium for *in vivo* fluorescence assays. The antibiotics used were 100 μg ml^{-1} carbenicillin (Fisher) and 34 μg ml^{-1} chloramphenicol (Acros). Culturing, genetic transformation and verification of transformation were done as previously described[22], using either *AmpR* or *CmR* as selection markers. Low-salt (5 g/l) Luria Broth medium (Sigma) was used for *in vivo* fluorescence assay of *B. subtilis* cells, with a chloramphenicol resistance gene as the selection marker. Drop-out Mix Synthetic Complete Medium (US Biological) was used for *in vivo* fluorescence assay of *S. cerevisiae* cells, with uracil and methionine as auxotrophic selectable markers.

Plasmid construction. The Csy4 gene from *P. aeruginosa* UCBPP-PA14 (NCBI Reference Sequence accession number YP_790814) was cloned from the previously described pHMGWA-Csy4 vector[3] using primers 5′-TTCAAAAGATCTAAAGAGGAGAAAGGATCTATGGACCACTACCTCGACATTCGCTTGCGA-3′ and 5′-TCCTTACTCGAGTTATCAGAACCAGGGAACGAAACCTCC-3′, and inserted into a vector containing a tetracycline-inducible promoter $P_L$tetO-1 (ref. 30), an ampicillin-selectable marker and a ColE1 replication origin (pCsy4). A second vector containing a chloramphenicol-selectable marker and a pSC101 replication origin (low copy) was used for cloning reporter constructs without or with the 28-nt Csy4 cleavage sequence (5′-GTTCACTGCCGTATAGGCAGCTAAGAAA-3′) following standard cloning techniques (pControl library and pCRISPR library). In the case of complex *cis*-regulatory circuits, the vector containing a chloramphenicol-selectable marker and a p15A replication origin was used. Detailed cloning procedure for each experiment is described in **Supplementary Methods**.

Time-course measurements. The *E. coli* strain expressing the Csy4 protein, Top10-Csy4, was derived by transforming *E. coli* Top10 cells with pCsy4. Reporter plasmids were then transformed into the Top10-Csy4 cells, and cells were plated on LB-agar plates containing 100 μg ml^{-1} carbenicillin and 34 μg ml^{-1} chloramphenicol, followed by incubation at 37 °C overnight. For the strains with random 30-nt UTRs, one single colony with a unique 30-nt UTR insertion (verified by sequencing) was picked. In all other experiments, three single colonies of each construct were picked. The picked colonies were grown in 300 μl of EZ-RDM containing 100 μg ml^{-1} carbenicillin and 34 μg ml^{-1} chloramphenicol in 2-ml 96-well deep-well plates (Costar 3960) overnight at 37 °C and 1,000 r.p.m. in a high-speed Multitron shaker (ATR). One microliter of this overnight culture was then added to 149 μl of fresh EZ-RDM with the same antibiotic concentrations with or without 2 μM anhydrotetracycline (Fluka). Fluorescence expression from the lag growth phase to the stationary phase was monitored using a high-throughput fluorescence plate reader (Tecan M1000) for 24 h. The excitation and emission wavelengths used for superfolder GFP (sfGFP) were 485 nm and 510 nm; they were 587 nm and 610 nm for mRFP; optical densities were measured at 600 nm (OD_{600}); the shaking period between consecutive measurements was 900 s with the shaking diameter of 2.5 mm.

Flow cytometry and analysis. Flow cytometry measurements were carried out as previously described[22]. The 300-μl cell cultures were grown to an OD_{600} of 0.3 in a Multitron shaker before measurement. Cells were sampled with a medium flow rate until 80,000 cells had been collected. Data were analyzed using FCS Express (*De novo* Software) by gating on a polygonal region containing 75% cell population in the forward scatter-side scatter plot.

Testing Csy4 cleavage in different organisms. The gram-negative bacterium *E. coli* K12 strain Top10, the gram-positive bacterium *B. subtilis sp.* 168 and the eukaryotic organism *S. cerevisiae* strain BY4741 were used. Three reporter systems with similar architecture were constructed by inserting a 30-nt Csy4 cleavage site (5′-AGTTCACTGCCGTATAGGCAGCTAAGAAAT-3′) in-frame between the ATG start codon and downstream reporter protein-coding sequence. The *E. coli* reporter system consisted of a J23119 promoter, a Bujard RBS and the sfGFP coding gene. The *B. subtilis* reporter system consisted of a hyperspank promoter (http://partsregistry.org/Part:BBa_K143054), a consensus *B. subtilis* RBS (5′-GGATCTAAGGAGGAAGGATCT-3′) and a GFP coding gene (GFPmut3). The yeast reporter system consisted of a strong pTDH3 promoter and a Venus coding gene (a mutant of yellow fluorescent protein)[31]. Time-course fluorescence of these reporter systems was assayed in their host cells with and without Csy4 co-expression as described. Protein production rates of three colonies were measured. The cells were visualized with a microscope (Zeiss, Axio Observer D1). In all cases, Csy4 cleavage led to almost complete reporter gene silencing owing to removal of the Shine-Dalgarno sequence and ATG start codon for *E. coli* and *B. subtilis*, or owing to removal of the 5′ m7G capping and ATG start codon for *S. cerevisiae* (**Fig. 3d**,**e**).

Northern blot analysis. Single colonies containing indicated genomic UTR-GFP reporter construct with or without Csy4 co-expression were grown in 5 ml EZ-RDM containing 100 μg ml^{-1} carbenicillin, 34 μg ml^{-1} chloramphenicol and 2 μM anhydrotetracycline. Samples were pelleted by centrifugation at OD_{600} of 0.6 to ~0.7. Total RNA was extracted using the mirVana miRNA Isolation Kit (Ambion) per manufacturer's instructions. We separated 5 μg of each total RNA sample by electrophoresis on a 9% urea polyacrylamide gel. Samples were subsequently transferred to a nylon membrane (Hybond-N+, GE Healthcare) using a semi-dry transfer cell (Bio-Rad). The membrane was pretreated with ULTRAHyb-Oligo Hybridization Buffer (Ambion) and probed overnight with a 5′-^{32}P–radiolabeled DNA oligonucleotide complementary to the *GFP* open reading frame (5′-CTTCAGCACGCGTCTTGTAGGTCCCGTCATC-3′). The membrane was washed twice with 2× saline-sodium citrate (SSC) buffer containing 0.5% SDS and visualized by phosphorimaging. The probe was stripped from the membrane by rocking the membrane in 200 ml of preboiled 0.1% SDS at 66C for 20 min. The membrane was pretreated with hybridization buffer again and then probed with a 5′-^{32}P–radiolabeled DNA oligonucleotide complementary to 16S ribosomal RNA (5′-CGTCAATGAGCAAAGGTATTAACTTTACTCCCTTCCTCCCCGC-3′). After washing with 2× SSC as before, the membrane was visualized by phosphorimaging.

Calculation of protein production rates. Protein production rates (PPRs) were calculated using the equation[32]

$$PPR = \left.\frac{\partial F}{\partial OD}\right|_{SS} \cdot \mu \cdot \left(1 + \frac{\mu}{\nu}\right)$$

where F is fluorescence, ν is protein maturation rate (per hour) and μ is growth rate (per hour). For each construct, we measured the temporal curves of F and OD_{600}. The plot of the measured fluorescence F as a function of OD_{600} showed a linear curve for all circuits tested during the exponential growth phase, which allowed us to calculate the slopes of this linear curve

$$\left.\frac{\partial F}{\partial OD}\right|_{ss}$$

We calculated μ during the exponential phase for each construct by plotting $\log(OD_{600})$ over time. The maturation constants for sfGFP and mRFP were $m_{sfGFP} = 7\ h^{-1}$ (ref. 33) and $m_{mRFP} = 3.5\ h^{-1}$ (ref. 34). Data were analyzed using Mathematica 7 (Wolfram).

Statistical analysis. The statistical significance (P value) used to compare the distribution of samples with or without RNA processing (**Fig. 1b**–**d**) was determined using two-tailed Student's t-test (Prism 5, GraphPad Software). The Spearman's rank correlation coefficients (**Fig. 1f** and **Supplementary Fig. 5**) were calculated using Microsoft Excel.

30. Lutz, R. & Bujard, H. Independent and tight regulation of transcriptional units in *Escherichia coli* via the LacR/O, the TetR/O and AraC/I1–I2 regulatory elements. *Nucleic Acids Res.* **25**, 1203–1210 (1997).
31. Nagai, T. *et al.* A variant of yellow fluorescent protein with fast and efficient maturation for cell-biological applications. *Nat. Biotechnol.* **20**, 87–90 (2002).
32. Leveau, J.H. & Lindow, S.E. Predictive and interpretive simulation of green fluorescent protein expression in reporter bacteria. *J. Bacteriol.* **183**, 6752–6762 (2001).
33. Pédelacq, J.-D., Cabantous, S., Tran, T., Terwilliger, T.C. & Waldo, G.S. Engineering and characterization of a superfolder green fluorescent protein. *Nat. Biotechnol.* **24**, 79–88 (2006).
34. Campbell, R.E. *et al.* A monomeric red fluorescent protein. *Proc. Natl. Acad. Sci. USA* **99**, 7877–7882 (2002).